

Photon distillation schemes with reduced resource costs based on multiphoton Fourier interference

F. H. B. Somhorst,¹ B. K. Sauër,¹ S. N. van den Hoven,¹ and J. J. Renema^{1,*}

¹MESA+ Institute for Nanotechnology, University of Twente, P. O. box 217, 7500 AE Enschede, The Netherlands

Improving the indistinguishability of single photons is a crucial prerequisite for achieving large-scale photonic quantum computation. Photon distillation uses quantum interference to enhance the quality of single photons, sacrificing multiple photons to generate one photon with enhanced indistinguishability. By studying multiphoton interference in Fourier matrices, we find photon distillation schemes that require fewer photons to achieve the same improvement in indistinguishability, compared to the state of the art. These results may find application as a component in large-scale photonic quantum computers.

I. INTRODUCTION

Achieving quantum computation beyond the NISQ era requires large-scale, error-corrected devices [1]. Progress towards fault-tolerant quantum computing is achieved both by reducing physical noise and by improving quantum-error correction schemes to relax threshold requirements. However, physical noise mechanisms are hardware-dependent, thereby requiring mitigation strategies specific to a particular computational platform.

Since the introduction of the Knill-Laflamme-Milburn scheme, linear optics stands out as a promising hardware platform for fault-tolerant photonic quantum computing [2]. In linear optics, allowable operations are restricted to measurement, linear optical circuits, i.e. optical devices which act linearly on the electric field amplitude, and classical reconfiguration of such circuits based on earlier measurement outcomes. Modern efforts center on fusion-based quantum computing (FBQC) [3–5], a computational architecture where multiple fixed-size entangled states - resource states - are entangled by fusion measurements. Recent experimental progress, for example in experimentally generating noisy three-qubit entangled states [6–8], shows the potential of this protocol.

The key resource for all linear-optical quantum computing schemes is photon indistinguishability [9–11], i.e. the degree to which the photons in the quantum computer are identical in the degrees of freedom of those photons which are not being used to encode information. The reason for the importance of indistinguishability as a resource is that while linearity forbids an explicit photon-photon interaction, it allows for multi-particle quantum interference, which is sufficient for universal quantum computation when combined with measurements and fast feedback. The archetypal example of multi-particle interference is the Hong-Ou-Mandel effect [12]. Since photon indistinguishability governs the degree to which multi-particle interference occurs, it is the crucial resource for photonic quantum computing in its modern implementations [13–16].

Photon distillation works by injecting multiple photons into a linear optical circuit and performing a measurement on some fraction of the outputs of that circuit. Conditional on observing a pre-defined measurement outcome (the herald) in all but one

of the outputs of the circuit, the remaining output is projected onto a state with improved photon indistinguishability. To improve the degree of indistinguishability of photons, photonic distillation schemes [17, 18] have been proposed and experimentally demonstrated [19]. Photon distillation (see Fig. 1) is a nondeterministic method for heralding indistinguishable photons. These schemes trade numbers for quality, exchanging multiple weakly indistinguishable photons for one photon with reduced distinguishability error, analogous to magic state distillation [20]. However, in contrast to conventional filtering, e.g. spectrally, photon distillation does not require prior knowledge about the target wave function of the indistinguishable photons. Moreover, photon distillation filters in all internal degrees of freedom simultaneously.

The resource cost C of such schemes is given by the number of photons of a given degree of indistinguishability that is on average required to obtain one photon of a given improved indistinguishability, or equivalently, the degree of improvement that can on average be achieved with a fixed number of photons. This resource cost, in turn, is determined by two factors: the *error reduction* R , i.e. the degree to which a single successful application of the scheme reduces the indistinguishability error on each photon, and the *heralding probability* p , i.e. the probability with which the scheme succeeds in the first place. In the limit of low errors, the error reduction reduces to a multiplicative factor, i.e. $\epsilon' = \epsilon/R$, where ϵ and ϵ' are the degree of error before and after the protocol, respectively. The probabilistic nature of the scheme can be mitigated by multiplexing [21], and for schemes where the available error reduction is limited, further error reduction is available by concatenation, i.e. using the input from one distillation step as input for the next. The current state-of-the-art photon distillation protocol is presented in Ref. [18], with a degree of error reduction of $R = 3$ and a heralding success probability $p = \frac{1}{3}$. This scheme requires concatenation and therefore has a resource cost quadratic in the overall error reduction required.

In this work, we demonstrate distillation methods for single photon state purification that have a lower resource cost than the state-of-the-art. We recognize that the scheme proposed in [18], originally found by numerical optimization, in fact implements a Fourier transform on the optical modes. Following on this observation, we both numerically and theoretically study Fourier-based distillation schemes with arbitrary numbers of photons, using simulation techniques originally designed for boson sampling [10, 22–25]. We find that

* j.j.renema@utwente.nl

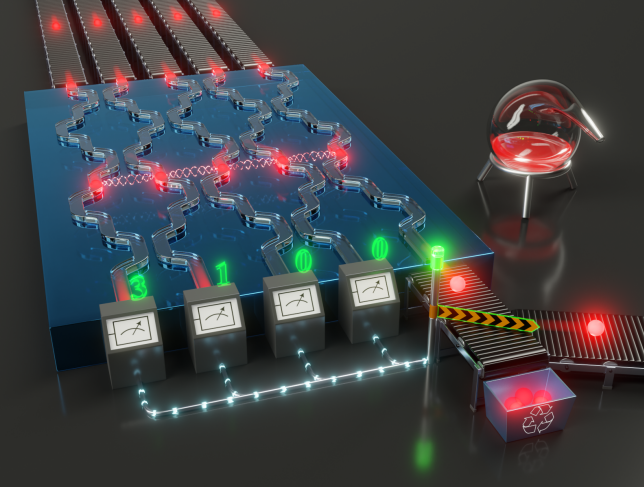


FIG. 1. **Artist's impression of photon distillation.** Partially distinguishable photons emitted by imperfect sources are interfered by a photonic distillation circuit. A given set of partial measurements heralds a quantum state with increased partial distinguishability. After a successful distillation attempt, this purified photon is ready to be processed for fusion based quantum computing. The distillation step reduces physical noise levels, which is important to achieve quantum error correction thresholds.

larger Fourier matrices give rise to more resource-efficient distillation schemes, compared to the scheme of [18]. This is due to the fact that for 5-mode Fourier transformations and larger, multiple detection outcomes herald a successful distillation step. Up to a conjecture in the theory of permanents of Fourier matrices, we find strong evidence that the probability of heralding success tends to a constant as a function of system size. This, combined with improved error reduction at larger system sizes, removes the need for concatenation, changing our resource cost from quadratic in the desired error reduction to linear. Besides studying the scaling in the limit of large numbers of photons, we discuss how our results can be implemented in systems of finite size. Our work contributes to the design of fault-tolerant photonic quantum computing architectures by cutting down resource costs for fault-tolerant photonic quantum computing.

Note added. - Related work was simultaneously published [26].

II. INTERFERENCE OF PARTIALLY DISTINGUISHABLE PHOTONS

We begin by introducing a model for partially distinguishable photons. The *orthogonal bad-bit model* describes single photon states produced by imperfect sources [17]. The internal error modes do not contribute to multiphoton interference because of their mutual orthogonality, thus allowing us to expand the imperfect single photon states $\rho(\epsilon)$ into equivalent sums of fully indistinguishable ρ_i and fully distinguishable ρ_d photons [25]

$$\rho(\epsilon) = (1 - \epsilon)\rho_i + \epsilon\rho_d, \quad (1)$$

where ϵ is the parameter used in this work for the partial distinguishability error [27]. A combination of an optical transformation plus partial measurement which projects onto a single photon state $\rho(\epsilon')$ results in photon distillation when $\epsilon' < \epsilon$.

In linear quantum optics, optical transformations U are implemented as a linear transformation acting on the bosonic modal creation operators $(\hat{a}_1^\dagger, \dots, \hat{a}_N^\dagger)^T \mapsto U(\hat{a}_1^\dagger, \dots, \hat{a}_N^\dagger)^T$, with U a unitary matrix. In state space representation, the imperfect multiphoton state transforms to

$$\rho(\epsilon)^{\otimes N} \mapsto \sigma(\epsilon) := U(U)\rho(\epsilon)^{\otimes N}U(U)^\dagger. \quad (2)$$

Where $U(U)$ is the state space transformation induced by the modal transformation U [28]. For given partial measurements in photon number basis, we project the remaining mode N into the state

$$\rho(\epsilon') = \mathcal{N}^{-1} \langle n_1, \dots, n_{N-1} | \sigma(\epsilon) | n_1, \dots, n_{N-1} \rangle, \quad (3)$$

with normalization $\mathcal{N} = \text{tr}[\langle n_1, \dots, n_{N-1} | \sigma(\epsilon) | n_1, \dots, n_{N-1} \rangle]$. Here we have assumed (as is the case in experiments) that the internal quantum state of the photons in modes $1, \dots, N-1$ cannot be resolved. Because U conserves photon number, the state in the remaining mode is projected into a definite photon number. Particularly, if the condition $\sum_{i=1}^{N-1} n_i = N-1$ is obeyed, the state is projected onto a single photon, with an internal state $\rho(\epsilon')$ which can be computed from Eq. 3.

Finally, we observe that for sufficiently low partial distinguishability error ϵ , the input state can be approximated as

$$\rho(\epsilon)^{\otimes N} = (1 - N\epsilon)\rho_i^{\otimes N} + \epsilon \sum_{k=1}^N \rho_i^{\otimes k-1} \otimes \rho_d \otimes \rho_i^{\otimes N-k} + \mathcal{O}(\epsilon^2). \quad (4)$$

In App. A we derive that this first-order error approximation is valid for photon distillation if $\delta_N(\epsilon) \ll \epsilon$, where $\delta_N(\epsilon) := 1 - (1 - \epsilon)^N - N\epsilon(1 - \epsilon)^{N-1}$ is the probability of higher-order errors in the input state.

Next, we recall some facts about Fourier transformations in linear optics. For a Fourier transformation, the matrix elements of U read:

$$U_{jk} := \frac{1}{\sqrt{N}} e^{i2\pi(j-1)(k-1)/N}. \quad (5)$$

Such transformations have been studied extensively [29–36] in quantum optics, since their high degree of symmetry offers various attractive properties. In particular, when a single, fully indistinguishable photon is present in each input mode, the output distribution of a Fourier matrix obeys the *zero-transmission law*, where all outcomes which have

$$\sum_{k=1}^N m_k \bmod N \neq 0, \quad (6)$$

are never observed [29], where $m = (m_1, \dots, m_N)$ is the equivalent ordered mode-assignment list corresponding to a

particular measurement $|n_1, \dots, n_N\rangle\langle n_1, \dots, n_N|$ [37]. Such outcomes are referred to as *forbidden outcomes*, and we will refer to the complementary set of these outcomes as *allowed outcomes* [38]. The fact that occurrence of these outcomes can be predicted efficiently despite the fact that computing the probability of a particular outcome of a linear optical circuit is in general computationally hard, combined with the fact that distinguishable photons do not obey the zero-transmission law, makes Fourier matrices an attractive probe for photon distinguishability in experiments. Moreover, straightforward numerical optimization of the task of estimating photonic indistinguishability results in either Fourier matrices or combinations of Fourier matrices being the optimal choice of matrix settings, depending on the precise specifications of the task [33].

III. FOURIER TRANSFORM-BASED DISTILLATION

In the previous section, we established the framework for imperfect photon interference. To establish intuition for the problem of purification in Fourier matrices, we first extensively study the $N = 5$ photon Fourier transform with a single photon at each input mode, in both error reduction and heralding probability. A detailed description of our numerical simulation methods is presented in App. B.

Fig. 2 shows the error reduction as a function of input error, for different partial measurement outcomes on modes 1 through 4. Surprisingly, there is more than one valid herald measurement for successful photon distillation. We observe three distinct families of successful heralding patterns.

We observe a correspondence between allowed outcomes following Eq. 6 and herald patterns which correspond to photon distillation: every herald pattern which enables photon distillation corresponds to an allowed outcome. In the limit of small initial error (see inset of Fig. 2), we find an error reduction $\epsilon' = \frac{\epsilon}{5} + \mathcal{O}(\epsilon^2)$ for all distinct herald measurements, accurate to the numerical precision of our computations.

Fig. 3 shows the heralding probabilities associated with each family of distillation outcomes. For asymptotically low initial error, we find a total herald probability of $p = \frac{33}{125} + \mathcal{O}(\epsilon)$, divided over many heralding outcomes. This breaks the previously conjectured $p = \frac{1}{N} + \mathcal{O}(\epsilon)$ scaling [18] coming from a single outcome. We strengthen our observations at $N = 5$ by numerical simulations up to $N = 10$. We find error scaling of $\epsilon' = \frac{\epsilon}{N} + \mathcal{O}(\epsilon^2)$, while simultaneously a total herald success probability of $p \geq \frac{1}{4} + \mathcal{O}(\epsilon)$ is observed [39]. A phenomenon which occurs at higher N which is not observed at $N = 5$ is that there are allowed outcomes which nonetheless have zero output probability - a consequence of the fact that Eq. 6 is a necessary but not sufficient condition.

IV. THEORETICAL ANALYSIS

We now concentrate on studying the limit of low partial distinguishability error. The following three key facts, valid in the limit of low error, emerge from our numerical study:

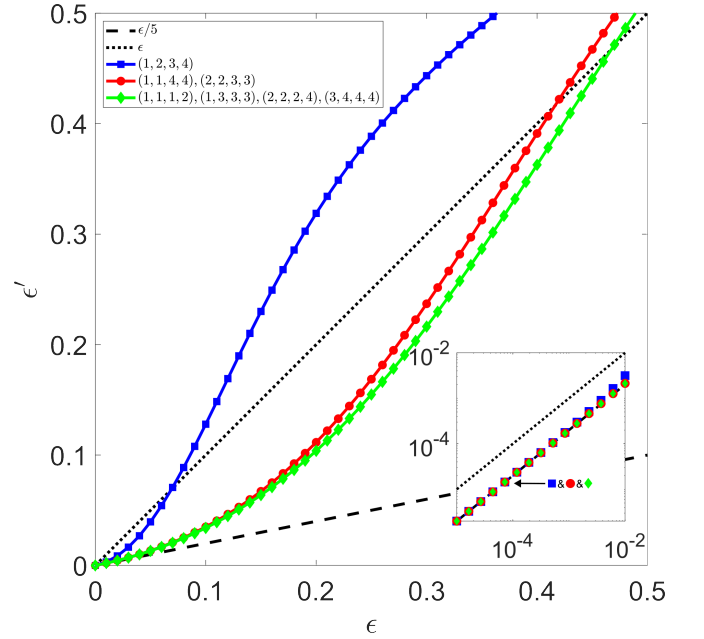


FIG. 2. **Error reduction for the 5-photon Fourier transform-based distillation scheme.** One photon with partial distinguishability error ϵ' is distilled out of $N = 5$ photons with initial error ϵ . Here, the legend indicates (ordered) herald measurement mode-assignment lists (m_1, m_2, m_3, m_4) that specify how the remaining 4 photons are distributed among the first 4 modes, where the distilled photon is in mode 5. All other measurements result in a failure of the distillation scheme. The distillation process only works when ϵ is below a herald measurement-dependent threshold. *Inset* Zoom-in to the low error regime, on a double-logarithmic scale. In this regime, we observe identical linear behaviour for all distillation patterns.

- The error reduction tends to $\epsilon' = \epsilon/N$ for valid herald patterns.
- Every allowed outcome which has precisely 1 photon in the desired optical mode constitutes a valid partial measurement for distillation.
- The total herald success probability tends to $\frac{1}{4}$ in the limit of large N .

In this section, we will provide our evidence for these assertions. We will prove the first two claims up to a technical conjecture in the theory of permanents of Fourier matrices, and give numerical and heuristic evidence for the third. In the next section, we will discuss the implications of these results for the design of distillation schemes in photonic quantum computers.

We will first focus on the error reduction. In the orthogonal bad-bit model, we have a classical mixture of states containing various error contributions, and error reduction is most easily understood in a Bayesian context: the posterior probability of our state containing zero errors after a partial measurement is given by:

$$P(\rho_i^{\otimes N} | M) = \frac{q_i}{q(\epsilon)} \cdot P(\rho_i^{\otimes N}). \quad (7)$$

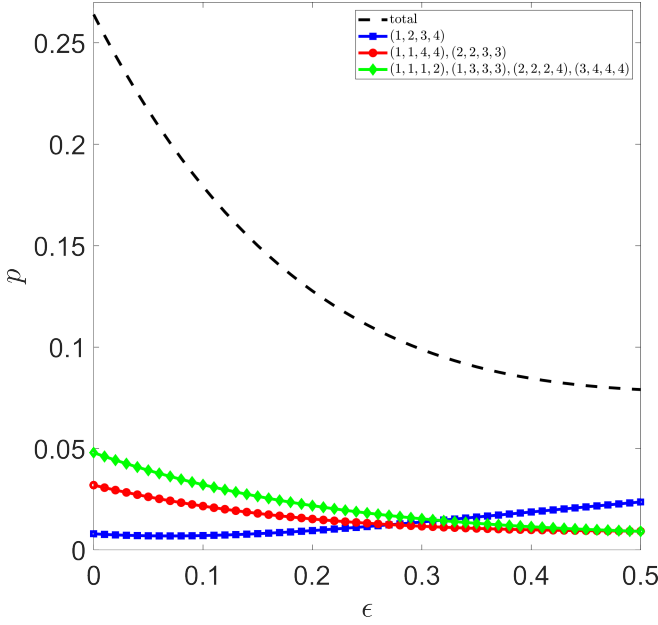


FIG. 3. **Herald probability for the 5-photon Fourier transform-based distillation scheme.** This figure shows the herald probability p as a function of partial distinguishability error ϵ . The legend indicates (ordered) herald measurement mode-assignment lists (m_1, m_2, m_3, m_4) that specify how the remaining 4 photons are distributed among the first 4 modes, while the distilled photon is in mode 5. The dashed line plots the total herald probability, which is larger than $1/4$ in the low error regime.

where $q(\epsilon)$ is the probability of obtaining that measurement outcome as a function of the error probability, and q_i is the probability of obtaining that measurement outcome for fully indistinguishable photons. This implies that if we observe a partial measurement outcome which is more likely to occur when the state contains zero errors, then we increase the posterior probability that the parts of our state which remain correspond to the part that contains zero errors. We are therefore looking for partial measurements where the probability of observing that outcome $q(\epsilon)$ is a strongly decreasing function of the error probability.

To compute the probability of a measurement outcome as a function of the probability of an error, we use the formalism of Refs. [23, 24]. In this formalism, multiphoton interference is split up into terms corresponding to quantum interference of j photons and classical transmission of the remaining $N - j$ photons, summed over all partitions into interfering and non-interfering photons. The probability of a single given herald measurement outcome is then given by

$$q(\epsilon) := \sum_{j=0}^N c_j (1 - \epsilon)^j, \quad (8)$$

where c_j sums up the contributions from all j -photon interference contributions [24].

For small partial distinguishability error, we approximate

Eq. 8 as:

$$q(\epsilon) = \sum_{j=0}^N c_j - \epsilon \sum_{j=0}^N c_j j + \mathcal{O}(\epsilon^2), \quad (9)$$

where $q_i = \sum_{j=0}^N c_j$ is the measurement probability for fully indistinguishable photons.

We now introduce our conjecture: for Fourier matrices fed with single photons, we find that the identity

$$\sum_{j=0}^N c_j j = (N - 1) \sum_{j=0}^N c_j. \quad (10)$$

holds. We have numerically tested this conjecture for $N = 3$ through $N = 10$ (App. C, Tab. I) and find that it holds to within the numerical precision of our calculations.

We use Eq. 10 to write

$$q(\epsilon) = q_i - \epsilon(N - 1)q_i + \mathcal{O}(\epsilon^2). \quad (11)$$

Combining this with (Eq. 4)

$$q(\epsilon) = q_i(1 - N\epsilon) + \lambda N\epsilon + \mathcal{O}(\epsilon^2), \quad (12)$$

where λ is the conditional probability of measuring a given herald measurement outcome given that one of the photons is distinguishable, we find $\lambda = q_i/N$. Using a similar approach as Ref. [18], we find for the new error ϵ'

$$1 - \epsilon' = \frac{(1 - N\epsilon) \cdot q_i \cdot 1 + N\epsilon \cdot \lambda \cdot \frac{N-1}{N}}{(1 - N\epsilon)q_i + N\epsilon \cdot \lambda} = 1 - \frac{\epsilon}{N} + \mathcal{O}(\epsilon^2), \quad (13)$$

which confirms the observed $\epsilon' = \frac{\epsilon}{N} + \mathcal{O}(\epsilon^2)$ scaling for Fourier transform-based distillation schemes.

Next, we note that this calculation directly implies that each allowed outcome with exactly 1 photon in the desired optical mode corresponds to a valid heralding pattern within the low error approximation. Eq. 11 shows that the probability of observing any allowed outcome M either a) always decreases with increasing error, in which case the allowed outcome constitutes a distillation strategy or b) always remains zero up to $\mathcal{O}(\epsilon^2)$ in case of allowed outcomes which have $p = 0$, which is never observed in experiment in the parameter regime under consideration here. For this reason the posterior probability of there not being any errors in the state must increase after such a measurement.

We remark that our conjecture sheds some light on why Fourier matrices repeatedly emerge as such useful tools for measuring and controlling partial distinguishability: Eq. 10 also holds trivially for outcomes where all photons emerge from the same mode, in any interferometer, whereas we find that for general outcomes Haar-random interferometers, it does not hold. Outcomes where all photons emerge from the same mode exhibit bosonic bunching, which is a multiphoton constructive interference phenomenon that strongly modifies the output distribution of indistinguishable particles. However, in any interferometer, bunched outcomes only occur with

a small probability, which moreover decreases as a function of system size [40]. In a Fourier matrix, in contrast, in the low error regime, our results show that all outcomes behave as if they corresponded to bunched outcomes. We leave this point for future study.

Finally, we focus on computing the total success probability of our scheme. We carry out two approaches. First, we perform a full computation of $p := \sum q_i$, valid for all N . We explicitly compute p by adopting the extended sample space formalism of Clifford & Clifford [41] to find (full derivation in App. D)

$$p = \sum_{j=0}^N (-1)^j (j+1) \prod_{i=1}^j \left(1 - \frac{i}{N}\right). \quad (14)$$

This formula holds for all N , but the alternating nature of the terms makes computation of an asymptote nontrivial. Numerical computations up to $N = 1000$ show that the condition $p \geq \frac{1}{4}$ holds in that regime, with an apparent asymptote at $\frac{1}{4}$.

A second approach is concerned only with the limit of large N . We can make a few observations. First, we note that for any N , the symmetry properties of Fourier matrices mean that they obey the condition $\forall (l_i = m_i + 1 \bmod N) \rightarrow p_l = p_m$, where l and m are mode assignment lists. In other words, if all elements of two mode assignment lists differ by one, then the probabilities are equal. Secondly, the substitution $U_{i,j} = \bar{U}_{i,j}$, where the overbar represents the complex conjugate, results in a relabeling of the modes while not altering the permanent of submatrices of U . These two relations define equivalence classes in the space of outputs. Third, in the limit of large N , almost every allowed belongs to an equivalence class that also contains allowed outcomes which correspond to photon distillation, i.e. which have exactly one photon in the mode of interest. These considerations suggest that in the limit of large N , imposing the restriction that there is a single photon in mode N does not substantially modify the statistics of the subset of outcomes that arises as a result of imposing that condition. In other words, a sample of outcomes with this condition will have the same average value as a sample without this condition. In that case, a simple counting argument suffices to compute the limiting value of the success probability: there are $\binom{2N-1}{N}$ measurements in general of which a fraction $\frac{1}{N}$ satisfies the complementary of Eq. 6 [29]. Furthermore, there are $\binom{2N-3}{N-1}$ measurements in which there is exactly 1 photon in output mode N , of which a fraction $\frac{1}{N}$ satisfies the complementary of Eq. 6 too. We find a total herald probability

$$p = \frac{\frac{1}{N} \binom{2N-3}{N-1}}{\frac{1}{N} \binom{2N-1}{N}} = \frac{1}{4 - \frac{2}{N}} = \frac{1}{4} + \frac{1}{8N} + \mathcal{O}\left(\left(\frac{1}{N}\right)^2\right). \quad (15)$$

Then, it follows naturally that $\lim_{N \rightarrow \infty} p = \frac{1}{4}$. Our proof sketch explains the asymptotic behavior, but it underestimates the convergence scaling (App. D, Fig. 10 [42]), demonstrating the need for future work on this topic.

V. DISCUSSION

We first focus on performance metrics in the small error limit, i.e. in the regime where Eq. 4 is valid. We are specifically interested in the number of photons required for one purified photon of with error reduction $\frac{\epsilon}{\epsilon'}$. This improvement is obtained by either concatenating smaller distillation circuits or using larger distillation circuits in a single step. In either case, the photon resource cost is of the order $C = \mathcal{O}\left(\left(\frac{\epsilon}{\epsilon'}\right)^\gamma\right)$ [18]. For generalized N -photon Fourier transform-based distillation schemes, we obtained a one-step accuracy $\frac{\epsilon}{\epsilon'} = N$. Then, the scaling coefficient γ is given by

$$\gamma := 1 + \frac{\log_2 p^{-1}}{\log_2 N}. \quad (16)$$

Plugging in the asymptotic value of $\lim_{N \rightarrow \infty} p = \frac{1}{4}$ gives:

$$\gamma \leq 1 + \frac{2}{\log_2 N} \quad (17)$$

as an upper bound for the scaling coefficient for the scaling coefficient.

Fig. 4 shows γ as a function of N , both using an exact computation of p from Eq. 14, and using the upper bound. Eq. 17 only slightly overestimates the required number of photons for $N \geq 5$. Eq. 17 implies a transition from quadratic to linear scaling for sufficiently large N -photon Fourier transform-based distillation schemes. This transition ultimately arises because our results show that the optimal strategy in the small-error regime is to take as many photons as are necessary to achieve the error reduction target and interfere them in a single distillation step. Because that distillation step succeeds with constant probability independent of the system size, this is the optimal strategy. In particular, we find

$$\left(\frac{\epsilon}{\epsilon'}\right)^\gamma \leq \left(\frac{\epsilon}{\epsilon'}\right)^{\log_2 4} \cdot \left(\frac{\epsilon}{\epsilon'}\right). \quad (18)$$

Since $\epsilon/\epsilon' = N + \mathcal{O}(\epsilon^2)$, we find a linear resource cost scaling

$$C \leq \mathcal{O}\left(4 \left(\frac{\epsilon}{\epsilon'}\right) + \mathcal{O}(\epsilon^3)\right). \quad (19)$$

Next, we discuss the applicability of our results in the regime where Eq. 4 does not hold. In this regime, the error reduction depends on the specific heralding pattern, and therefore each heralding pattern has a different error threshold and error reduction, as can be seen in Fig. 2. It is therefore necessary to know both the input error of the photon and the function that describes the error reduction as a function of input error and herald pattern. Since these functions are polynomials in the error, but computing the coefficients of these polynomials is a computationally expensive task, and since very similar computations would have to occur many times in the same clock cycle in a photonic quantum computer, it makes sense to pre-compute the coefficients of these polynomials, or even to create a lookup table [43]. Furthermore, in this regime, it may be optimal to perform multiple

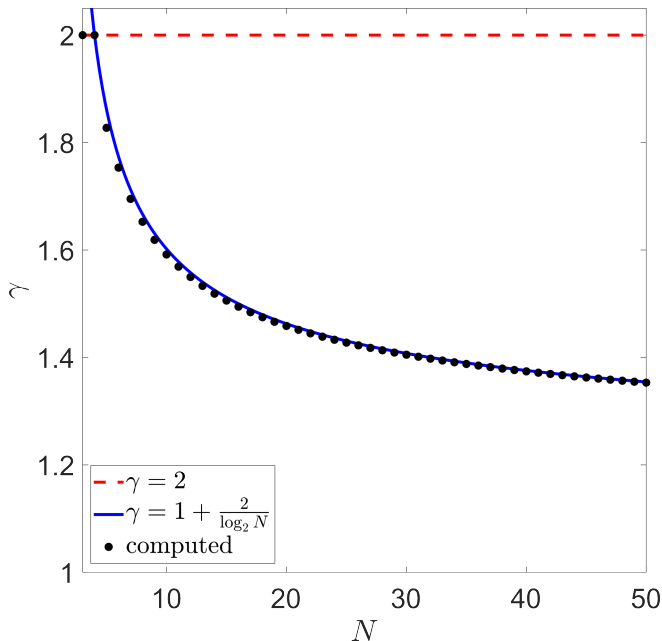


FIG. 4. **Resource cost scaling coefficient for N -photon Fourier transform-based distillation schemes.** The figure shows the parameter γ , which characterizes the resource cost, as a function of the number of photons N . In the limit of small partial distinguishability error, the required number of photons to distill one purified photon is $\mathcal{O}((\frac{\epsilon}{\epsilon'})^\gamma)$. The black symbols show the scaling coefficient γ as computed via direct computation. The blue line shows an upper bound (Eq. 17, blue line) which only slightly overestimates the exact calculations. $N = 3, 4$ follow the quadratic scaling law found in Ref. [18] (red dashed line).

distillation steps, since the convergence to a constant success probability cannot be guaranteed. Since in this regime, the error reduction cannot be predicted before each distillation step, the distillation protocol will have to be adaptive, relying on multiple possible routing schemes, which may themselves be pre-computed, to route the photons.

VI. CONCLUSION

In conclusion, we have used a combination of numerical and theoretical tools to shown that generalized Fourier

transform-based distillation schemes can be used to purify photons from imperfect sources. For this purpose, we explicitly simulated the error reduction for the $N = 5$ photon Fourier transform where we showed that there are different paths towards perfect photon indistinguishability. Within the limit of low partial distinguishability error, we have shown modulo a conjecture that the error reduction scales linearly with the number of photons employed in the distillation scheme N , while we have given numerical and theoretical evidence that the success probability tends to a constant, giving rise to linear scaling in the number of photons required to achieve a given error reduction.

Applicability of our work strongly depends on the availability of high-fidelity programmable photonic processors and fast optical switches. However, we note that processor size and fidelity of linear optical circuits are constantly improving [31, 44–48]. Our generalized schemes contribute to the development of adaptive purification circuits, where concatenation strategies are dependent on the actual herald measurements of each distillation step. While current advances in single photon source engineering continue to improve photon indistinguishability [49–52], we anticipate that photon distillation will aid in the task of creating the millions of almost fully indistinguishable photons necessary for photonic quantum computing.

ACKNOWLEDGEMENTS

We thank J. Timmerhuis for scientific discussions. We thank J. Saied and J. Marshall for helpful comments on our first draft of the manuscript. This research is supported by the Photonic Integrated Technology Center (PITC). This project has received funding from PhotonDelta National Growth Fund programme. This publication is part of the project At the Quantum Edge (VI.Vidi.223.075) of the research programme VIDI which is financed by the Dutch Research Council (NWO).

COMPETING INTERESTS

F.H.B.S, B.K.S, and J.J.R. are the inventors on a relevant patent application submitted by the University of Twente (Dutch patent application no. 2037489). The authors declare no other competing interests.

[1] E. T. Campbell, B. M. Terhal, and C. Vuillot, Roads towards fault-tolerant universal quantum computation, *Nature* **549**, 172 (2017).
[2] E. Knill, R. Laflamme, and G. J. Milburn, A scheme for efficient quantum computation with linear optics, *Nature* **409**, 46 (2001).
[3] D. E. Browne and T. Rudolph, Resource-efficient linear optical quantum computation, *Physical Review Letters* **95**, 010501 (2005).

[4] T. Rudolph, Why i am optimistic about the silicon-photonics route to quantum computing, *APL Photonics* **2**, 030901 (2017).
[5] S. Bartolucci, P. Birchall, H. Bombin, H. Cable, C. Dawson, M. Gimeno-Segovia, E. Johnston, K. Kieling, N. Nickerson, M. Pant, *et al.*, Fusion-based quantum computation, *Nature Communications* **14**, 912 (2023).
[6] S. Chen, L.-C. Peng, Y.-P. Guo, X.-M. Gu, X. Ding, R.-Z. Liu, X. You, J. Qin, Y.-F. Wang, Y.-M. He, *et al.*, Heralded three-photon entanglement from a single-photon source on a photonic

- chip, *Physical Review Letters* **132**, 130603 (2024).
- [7] H. Cao, L. Hansen, F. Giorgino, L. Carosini, P. Záhálka, F. Zilk, J. Loredó, and P. Walther, Photonic source of heralded greenberger-horne-zeilinger states, *Physical Review Letters* **132**, 130604 (2024).
 - [8] N. Maring, A. Fyrrillas, M. Pont, E. Ivanov, P. Stepanov, N. Margaria, W. Hease, A. Pishchagin, A. Lemaître, I. Sagnes, *et al.*, A versatile single-photon-based quantum computing platform, *Nature Photonics*, 1 (2024).
 - [9] L. Mandel, Coherence and indistinguishability, *Optics Letters* **16**, 1882 (1991).
 - [10] V. Shchesnovich, Sufficient condition for the mode mismatch of single photons for scalability of the boson-sampling computer, *Physical Review A* **89**, 022333 (2014).
 - [11] N. Lal, S. Mishra, and R. Singh, Indistinguishable photons, *AVS Quantum Science* **4**, <https://doi.org/10.1116/5.0083968> (2022).
 - [12] C.-K. Hong, Z.-Y. Ou, and L. Mandel, Measurement of subpicosecond time intervals between two photons by interference, *Physical Review Letters* **59**, 2044 (1987).
 - [13] P. Kok, W. J. Munro, K. Nemoto, T. C. Ralph, J. P. Dowling, and G. J. Milburn, Linear optical quantum computing with photonic qubits, *Reviews of modern physics* **79**, 135 (2007).
 - [14] J. L. O’Brien, Optical quantum computing, *Science* **318**, 1567 (2007).
 - [15] M. Varnava, D. E. Browne, and T. Rudolph, How good must single photon sources and detectors be for efficient linear optical quantum computation?, *Physical Review Letters* **100**, 060502 (2008).
 - [16] S. Slussarenko and G. J. Pryde, Photonic quantum information processing: A concise review, *Applied Physics Reviews* **6**, <https://doi.org/10.1063/1.5115814> (2019).
 - [17] C. Sparrow, *Quantum interference in universal linear optical devices for quantum computation and simulation*, Ph.D. thesis (2017).
 - [18] J. Marshall, Distillation of indistinguishable photons, *Physical Review Letters* **129**, 213601 (2022).
 - [19] C. F. D. Faurby, L. Carosini, H. Cao, P. I. Sund, L. M. Hansen, F. Giorgino, A. B. Villadsen, S. N. van den Hoven, P. Lodahl, S. Paesani, J. C. Loredó, and P. Walther, Purifying photon indistinguishability through quantum interference, *arXiv preprint arXiv:2403.12866* <https://doi.org/10.48550/arXiv.2403.12866> (2024).
 - [20] S. Bravyi and A. Kitaev, Universal quantum computation with ideal clifford gates and noisy ancillas, *Physical Review A* **71**, 022316 (2005).
 - [21] A. L. Migdall, D. Branning, and S. Castelletto, Tailoring single-photon and multiphoton probabilities of a single-photon on-demand source, *Physical Review A* **66**, 053805 (2002).
 - [22] V. Shchesnovich, Partial indistinguishability theory for multiphoton experiments in multiport devices, *Physical Review A* **91**, 013844 (2015).
 - [23] M. C. Tichy, Sampling of partially distinguishable bosons and the relation to the multidimensional permanent, *Physical Review A* **91**, 022316 (2015).
 - [24] J. J. Renema, A. Menssen, W. R. Clements, G. Triginer, W. S. Kolthammer, and I. A. Walmsley, Efficient classical algorithm for boson sampling with partially distinguishable photons, *Physical Review Letters* **120**, 220502 (2018).
 - [25] A. E. Moylett, R. García-Patrón, J. J. Renema, and P. S. Turner, Classically simulating near-term partially-distinguishable and lossy boson sampling, *Quantum Science and Technology* **5**, 015001 (2019).
 - [26] J. Saied, J. Marshall, N. Anand, and E. G. Rieffel, General protocols for the efficient distillation of indistinguishable photons, *arXiv preprint arXiv:2404.14217* <https://doi.org/10.48550/arXiv.2404.14217> (2024).
 - [27] The *orthogonal bad-bit model* is equivalent to the *partial distinguishability model* where $x := 1 - \epsilon$ [24]. The assumption of identical mutual partial distinguishability is demonstrated to be appropriate in multiphoton experiments with imperfect sources of sufficient quality [53].
 - [28] Arvind, B. Dutta, N. Mukunda, and R. Simon, The real symplectic groups in quantum mechanics and optics, *Pramana* **45**, 471 (1995).
 - [29] M. C. Tichy, M. Tiersch, F. de Melo, F. Mintert, and A. Buchleitner, Zero-transmission law for multiport beam splitters, *Physical Review Letters* **104**, 220405 (2010).
 - [30] M. C. Tichy, K. Mayer, A. Buchleitner, and K. Mølmer, Stringent and efficient assessment of boson-sampling devices, *Physical Review Letters* **113**, 020502 (2014).
 - [31] J. Carolan, C. Harrold, C. Sparrow, E. Martín-López, N. J. Russell, J. W. Silverstone, P. J. Shadbolt, N. Matsuda, M. Oguma, M. Itoh, *et al.*, Universal linear optics, *Science* **349**, 711 (2015).
 - [32] A. Crespi, R. Osellame, R. Ramponi, M. Bentivegna, F. Flamini, N. Spagnolo, N. Viggianiello, L. Innocenti, P. Mataloni, and F. Sciarrino, Suppression law of quantum states in a 3d photonic fast fourier transform chip, *Nature Communications* **7**, 10469 (2016).
 - [33] S. Stanisic and P. S. Turner, Discriminating distinguishability, *Physical Review A* **98**, 043839 (2018).
 - [34] C. Dittel, G. Dufour, M. Walschaers, G. Weihs, A. Buchleitner, and R. Keil, Totally destructive many-particle interference, *Physical Review Letters* **120**, 240404 (2018).
 - [35] D. J. Brod, E. F. Galvão, N. Viggianiello, F. Flamini, N. Spagnolo, and F. Sciarrino, Witnessing genuine multiphoton indistinguishability, *Physical Review Letters* **122**, 063602 (2019).
 - [36] F. H. B. Somhorst, R. van der Meer, M. Correa Anguita, R. Schadow, H. J. Snijders, M. de Goede, B. Kassenberg, P. Venderbosch, C. Taballione, J. Epping, *et al.*, Quantum simulation of thermodynamics in an integrated quantum photonic processor, *Nature Communications* **14**, 3895 (2023).
 - [37] For example, the mode-assignment list $(1, 2, 3, 4, 5)$ corresponds to the equivalent non-collision state $|11111\rangle$.
 - [38] However, a classification as *allowed outcome* is a necessary but not sufficient condition for a classification as *non-suppressed outcome*. Nevertheless, most allowed outcomes constitute non-suppressed outcomes [29].
 - [39] F. H. B. Somhorst, B. Sauër, S. van den Hoven, and J. Renema, "data underlying the manuscript: "photon distillation schemes with reduced resource costs based on multiphoton fourier interference", 4TU.ResearchData 10.4121/c0c83c18-f38b-46b8-b4f4-67964cb611d0 (2024).
 - [40] M.-H. Yung, X. Gao, and J. Huh, Universal bound on sampling bosons in linear optics and its computational implications, *National Science Review* **6**, 719 (2019).
 - [41] P. Clifford and R. Clifford, The classical complexity of boson sampling, in *Proceedings of the Twenty-Ninth Annual ACM-SIAM Symposium on Discrete Algorithms* (SIAM, 2018) pp. 146–155.
 - [42] J. Saied and J. Marshall, private communication.
 - [43] Pre-computed data for $N = 3$ to $N = 10$ can be found in [39].
 - [44] N. C. Harris, G. R. Steinbrecher, M. Prabhu, Y. Lahini, J. Mower, D. Bunandar, C. Chen, F. N. Wong, T. Baehr-Jones, M. Hochberg, *et al.*, Quantum transport simulations in a programmable nanophotonic processor, *Nature Photonics* **11**, 447 (2017).

- [45] C. Sparrow, E. Martín-López, N. Maraviglia, A. Neville, C. Harrold, J. Carolan, Y. N. Joglekar, T. Hashimoto, N. Matsuda, J. L. O'Brien, *et al.*, Simulating the vibrational quantum dynamics of molecules using photonics, *Nature* **557**, 660 (2018).
- [46] J. Wang, F. Sciarrino, A. Laing, and M. G. Thompson, Integrated photonic quantum technologies, *Nature Photonics* **14**, 273 (2020).
- [47] C. Taballione, R. van der Meer, H. J. Snijders, P. Hooijschuur, J. P. Epping, M. de Goede, B. Kassenberg, P. Venderbosch, C. Toebes, H. van den Vlekkert, *et al.*, A universal fully reconfigurable 12-mode quantum photonic processor, *Materials for Quantum Technology* **1**, 035002 (2021).
- [48] C. Taballione, M. C. Anguita, M. de Goede, P. Venderbosch, B. Kassenberg, H. Snijders, N. Kannan, W. L. Vleeshouwers, D. Smith, J. P. Epping, *et al.*, 20-mode universal quantum photonic processor, *Quantum* **7**, 1071 (2023).
- [49] N. Tomm, A. Javadi, N. O. Antoniadis, D. Najer, M. C. Löbl, A. R. Korsch, R. Schott, S. R. Valentin, A. D. Wieck, A. Ludwig, *et al.*, A bright and fast source of coherent single photons, *Nature Nanotechnology* **16**, 399 (2021).
- [50] H. Ollivier, S. Thomas, S. Wein, I. M. de Buy Wenniger, N. Coste, J. Lored, N. Somaschi, A. Harouri, A. Lemaitre, I. Sagnes, *et al.*, Hong-ou-mandel interference with imperfect single photon sources, *Physical Review Letters* **126**, 063602 (2021).
- [51] C. Becher, W. Gao, S. Kar, C. D. Marciniak, T. Monz, J. G. Bartholomew, P. Goldner, H. Loh, E. Marcellina, K. E. J. Goh, *et al.*, 2023 roadmap for materials for quantum technologies, *Materials for Quantum Technology* **3**, 012501 (2023).
- [52] X. Ding, Y.-P. Guo, M.-C. Xu, R.-Z. Liu, G.-Y. Zou, J.-Y. Zhao, Z.-X. Ge, Q.-H. Zhang, H.-L. Liu, M.-C. Chen, *et al.*, High-efficiency single-photon source above the loss-tolerant threshold for efficient linear optical quantum computing, *arXiv preprint arXiv:2311.08347* <https://doi.org/10.48550/arXiv.2311.08347> (2023).
- [53] J. J. Renema, H. Wang, J. Qin, X. You, C. Lu, and J. Pan, Sample-efficient benchmarking of multiphoton interference on a boson sampler in the sparse regime, *Physical Review A* **103**, 023722 (2021).
- [54] H. J. Ryser, *Combinatorial mathematics*, Vol. 14 (American Mathematical Soc., 1963).

Appendix A: Validity regime of first-order error approximation

Throughout our work, we work in the low-error regime, which we define as the regime where Eq. 4 holds, i.e. where at most one photon is in an error mode. Here, we point out that the regime over which this approximation is valid shrinks with increasing number of photons. The probability of measuring a product state where k out of N photons are indistinguishable is given by

$$P(k, N) = \binom{N}{k} (1 - \epsilon)^k \epsilon^{N-k}, \quad (\text{A1})$$

where $1 - \epsilon$ is the success probability as defined in Eq. 1. It follows that the 0-error probability is given by $P(0, N) = (1 - \epsilon)^N$ and the 1-error probability is given by $P(1, N) = N(1 - \epsilon)^{N-1}\epsilon$.

We define the probability of more-than-one error as

$$\delta_N(\epsilon) := \sum_{k=2}^N P(k, N). \quad (\text{A2})$$

Since the total probability is conserved, we find

$$\delta_N(\epsilon) := 1 - (1 - \epsilon)^N - N\epsilon(1 - \epsilon)^{N-1}. \quad (\text{A3})$$

To study photon distillation in the low error regime, we note that Eq. 4 is valid if the probability of having more than 1 error in a product state of N imperfect photons is (much) smaller than the partial distinguishability error in one imperfect photon, i.e. $\delta_N(\epsilon) \ll \epsilon$ or $\frac{\delta_N(\epsilon)}{\epsilon} \ll 1$. Fig. 5 provides a parametric plot of the fraction $\frac{\delta_N(\epsilon)}{\epsilon}$ as a function of N and ϵ . We observe that the validity range of ϵ shrinks with increasing N .

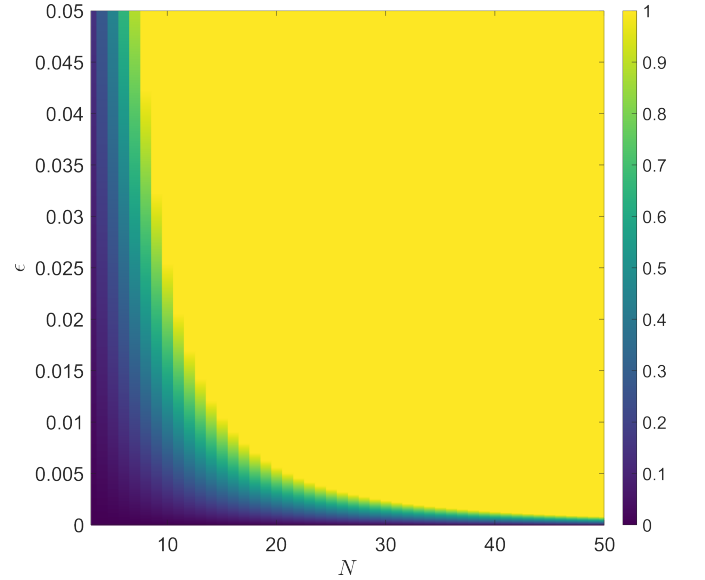


FIG. 5. **Parametric scan of single-error regime.** The figure shows the ratio of multi-error probability $\delta_N(\epsilon)$ over partial distinguishability error ϵ is plotted. The low-error approximation is valid in the regime where $\frac{\delta_N(\epsilon)}{\epsilon} \ll 1$. Note that $\frac{\delta_N(\epsilon)}{\epsilon} \geq 1$ is set to 1 to improve readability.

Appendix B: Simulation methods

Fig. 6 shows the optical circuit which we use to simulate photon distillation. The product state $\rho(\epsilon)^{\otimes N}$ is transformed by a N -mode Fourier transform into a multiphoton entangled state. A given partial measurement of the multiphoton output state in the first $N - 1$ modes heralds the presence of a single photon state $\rho(\epsilon')$ in mode N . Subsequently, the product state $\rho(\epsilon') \otimes \rho(\epsilon)$ is interfered by a balanced beam splitter. We extract the reduced partial distinguishability error ϵ' by computing first the new visibility $V' = (1 - \epsilon')(1 - \epsilon)$ for known ϵ . We compute the counting statistics behind the balanced beam splitter for a given herald measurement by using the formalism for interference of partially distinguishable photons

as presented in Ref. [23]. Our calculations assume perfectly functioning and loss-free components. Although studying the interference of two equally purified photons seems simpler, this actually requires the computation of matrix permanents of size $2N \times 2N$. Our setup only requires matrix permanent computations of size $(N+1) \times (N+1)$, which is beneficial because these computations are intrinsically inefficient [54].

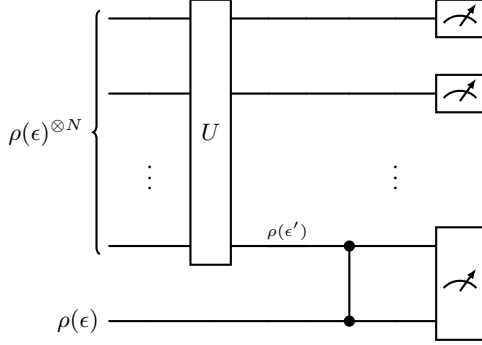


FIG. 6. **Distillation simulation setup.** N partial distinguishable photons are transformed by a N -mode Fourier transform U (Eq. 5) into a multiphoton state. The partial state in the first $N-1$ ancillary modes is measured. A successful measurement heralds the presence of a single photon state with reduced error $\epsilon' < \epsilon$ (Eq. 1) in mode N . The new error ϵ' is extracted by first evaluating the Hong-Ou-Mandel visibility of a distilled photon and a non-distilled photon by interference in a 50:50 beamsplitter. One unitary transformation matrix simultaneously describes all transformations to simulate the interference of $N+1$ partially distinguishable photons.

Appendix C: Multi-photon interference coefficients

The probability of output photon distribution i can be written in the formalism of Ref. [23, 24] as

$$q(\epsilon) := \sum_{j=0}^N c_j (1-\epsilon)^j, \quad (\text{C1})$$

where the j -th order multiphoton interference coefficients are defined by:

$$c_j := \frac{1}{\mu_i} \sum_{\sigma^j} \text{perm}[M \circ M_{\sigma^j}^*]. \quad (\text{C2})$$

Here, μ_i is a multiplicity correction $\mu(s) = \prod_i (s_i)!$ for outputs with more than one photon in the same mode, M is an N -by- N submatrix of unitary transformation matrix U (where rows and columns of M correspond to input and output modes, respectively), σ^j corresponds to all row permutations σ with $N-j$ fixed-point elements, \circ denotes the element-wise matrix product and $M_{\sigma^j}^*$ is the complex conjugate of the matrix M with rows permuted according to σ^j (for detail see [24]).

First, we analyze the c_j distribution of the $N=3$ photon distillation scheme proposed by Ref. [18]. We focus specifically on herald measurement list (1, 2), which corresponds to output photon distribution (1, 2, 3). The (normalized) coefficient distribution is presented in Fig. 7. We observe that the (absolute value of) 2- and 3-photon interference contributions are relatively high compared to the zero photon interference contribution c_0 , which corresponds to the transmission probability for fully distinguishable photons. By definition, $c_1 = 0$. One can verify $\sum_{j=0}^3 c_j j = 3c_0$ and $2 \sum_{j=0}^3 c_j = 3c_0$, so the $N=3$ Fourier transform-based distillation scheme satisfies Eq. 10.

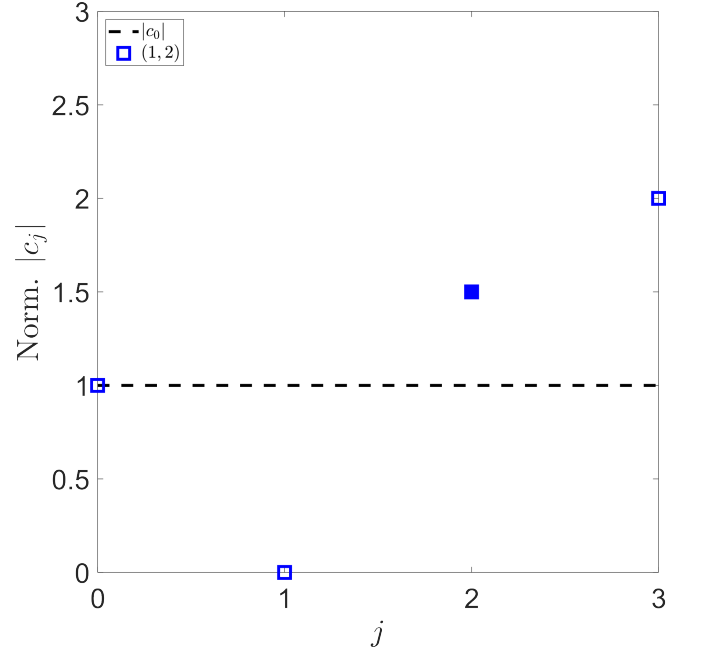


FIG. 7. **Multiphoton interference coefficients for the $N=3$ Fourier transform-based distillation scheme.** Absolute values of the j -th order multiphoton interference contribution coefficients c_j are plotted for herald measurement (1, 2). Open markers indicate a positive contribution while filled markers indicate a negative contribution. All coefficients are normalized with respect to c_0 , which is the probability of observing that detection event in case of fully distinguishable photons.

Now we turn our attention to the c_j distribution for the $N=5$ photon Fourier transform-based distillation scheme discussed in Sec. III, which is presented in Fig. 8. Similar to Fig. 7, the distribution for $N=5$ shows for all individual herald measurements the remarkable feature $\sum_{j=0}^5 c_j j = 4 \sum_{j=0}^5 c_j$ satisfying again Eq. 10. For reference, we have $\sum_{j=0}^5 c_j = \frac{5}{24}c_0$ (blue squares), $\frac{10}{3}c_0$ (red circles), $\frac{15}{2}c_0$ (green diamonds). Motivated by inspection of Fig. 2 and 3, we suspect that larger ratios $\sum_{j=0}^N c_j$ over c_0 indicate better performing photon distillation herald measurements.

For comparison, we inspected the c_j distribution for Haar-

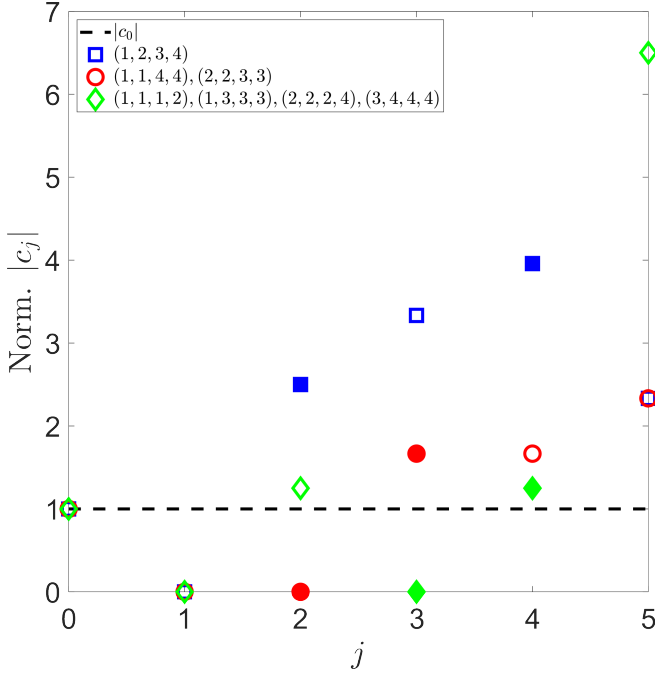


FIG. 8. **Multiphoton interference coefficients for the $N = 5$ Fourier transform-based distillation scheme.** Absolute values of the j -th order multiphoton interference contribution coefficients c_j are plotted for herald measurements $l_i = (m_1, m_2, m_3, m_4)$ that specify how the remaining 4 photons are distributed among the first 4 modes, while the distilled photon is in mode 5. Open markers indicate a positive contribution while filled markers indicate a negative contribution. All coefficients are normalized with respect to c_0 , which is the probability of observing that detection event in case of fully distinguishable photons.

random unitary matrices. We generate 10^4 Haar-random matrices and compute the ratio $\sum_{j=0}^N c_j j$ over $\sum_{j=0}^N c_j$ for all mode-assignment lists with exactly one in mode N . The histogram of this ratio, for $N = 3$ and $N = 5$ is plotted in Fig. 9. We observe that the herald measurements for the Fourier transforms (dashed and dotted lines) have extreme ratios that satisfy Eq. 10.

Finally, we summarize the results of our numerical studies for $N = 3$ through $N = 10$ in Tab. I. For each allowed outcome with exactly one photon in mode N , we calculated the multiphoton coefficients. For each of these allowed outcomes, we checked our conjecture (Eq. 10) by calculating the difference

$$\Delta := \left| \sum_{j=0}^N c_j j - (N-1) \sum_{j=0}^N c_j \right|, \quad (\text{C3})$$

which is ideally zero and which is a measure of the numerical accuracy of our calculations. Then, we calculated the number of allowed outcomes that are non-suppressed (and therefore relevant to photon distillation). In the case of $N = 6$ and $N = 10$ we find that some allowed outcomes have probability 0, which means they do not result in photon distillation, consistent with the results of Ref. [29].

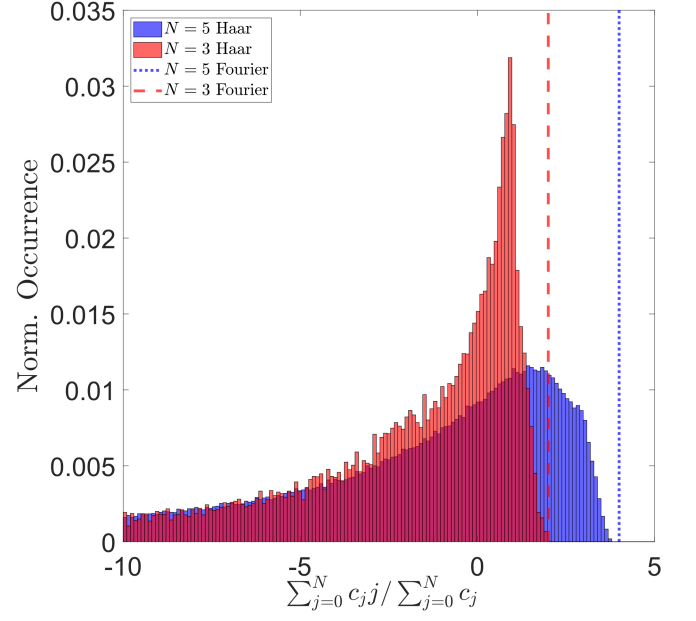


FIG. 9. **Multiphoton interference coefficients for Haar-random unitary transformations.** The normalized occurrence of the ratio $(\sum_{j=0}^N c_j j) / (\sum_{j=0}^N c_j)$ for all mode-assignment lists with exactly one photon in mode N for 10^4 random Haar matrices is presented for $N = 3, 5$. For comparison, the ratios calculated for relevant Fourier transform-based herald measurements are indicated by dashed/dotted lines.

Appendix D: Herald probability

To compute the total herald probability p , we focus on the marginal probability of observing exactly one photon in a particular mode of interest. Without loss of generality, we assume that the distilled photon is located in output mode 1. Using the expanded sample space formalism introduced by Clifford & Clifford [41], we focus first on the marginal probability where

TABLE I. **Summary of numerical analysis** for N -photon Fourier transform. Number of allowed outcomes where exactly one photon ends in mode N (N_{allowed}), maximum calculated numerical difference based on Eq. C3 (Δ_{max}), number of allowed outcomes that constitute a photon distillation strategy (N_{herald}), and percentage of allowed outcomes that constitute a photon distillation strategy.

N	N_{allowed}	Δ_{max}	N_{herald}	$N_{\text{herald}}/N_{\text{allowed}}$ (%)
3	1	0	1	100
4	2	$6 \cdot 10^{-17}$	2	100
5	7	$6 \cdot 10^{-17}$	7	100
6	20	$6 \cdot 10^{-17}$	14	70
7	66	$8 \cdot 10^{-16}$	66	100
8	212	$4 \cdot 10^{-17}$	212	100
9	715	$6 \cdot 10^{-16}$	715	100
10	2424	$2 \cdot 10^{-15}$	1944	80

the first k out of N photons end up in output mode 1:

$$p^{(k)} := p(1_1, \dots, 1_k). \quad (\text{D1})$$

According to Lemma 1 in Ref. [41], we find that the marginal probability of the subsequence $(1_1, \dots, 1_k)$ is given by

$$p^{(k)} = \frac{1}{k!} |\text{perm} M|^2, \quad (\text{D2})$$

where we used that, in case of Fourier transforms, all $\binom{N}{k}$ input - output combinations share the same submatrix M . Here, submatrix M is a rank 1 matrix of size $k \times k$ where the matrix elements are given by $M_{ij} = \frac{1}{\sqrt{N}}$ such that $\text{perm}(M) = \frac{k!}{\sqrt{N}^k}$. Therefore, we have

$$p^{(k)} = \frac{k!}{N^k}. \quad (\text{D3})$$

However, the marginal probability $p^{(k)}$ still includes the possibility that any of the $N - k$ leftover photons end in mode 1. We introduce the new marginal probability $\tilde{p}^{(k)}$ where none of the remaining $N - k$ photons end in mode 1, by definition. We can expand $p^{(k)}$ in terms of $\tilde{p}^{(k+j)}$ for $j \in \{0, 1, \dots, N - k\}$ such that the first $k + j$ photons are in output mode 1 while the leftover $N - k - j$ photons are excluded. For each j , there are $\binom{N-k}{j}$ equivalent probabilities. Therefore, we find

$$p^{(k)} = \sum_{j=0}^{N-k} \binom{N-k}{j} \tilde{p}^{(k+j)}. \quad (\text{D4})$$

Inversion of Eq. D4 results in

$$\tilde{p}^{(k)} = \sum_{j=0}^{N-k} (-1)^j \binom{N-k}{j} p^{(k+j)}. \quad (\text{D5})$$

For photon distillation purposes considered in this paper, we are interested in the particular case where $k = 1$. Substituting Eq. D3 in Eq. D5, we find

$$\tilde{p}^{(1)} = \frac{1}{N} \sum_{j=0}^{N-1} (-1)^j (j+1) \binom{N-1}{j} \frac{j!}{N^j}. \quad (\text{D6})$$

The last terms can be rewritten as

$$\binom{N-1}{j} j! = N^j \prod_{i=1}^j \left(1 - \frac{i}{N}\right), \quad (\text{D7})$$

such that

$$\tilde{p}^{(1)} = \frac{1}{N} \sum_{j=0}^{N-1} (-1)^j (j+1) \prod_{i=1}^j \left(1 - \frac{i}{N}\right). \quad (\text{D8})$$

As there are $\binom{N}{1} = N$ equivalent probabilities, we have $p = N\tilde{p}^{(1)}$. Therefore, we arrive at Eq. 14:

$$p = \sum_{j=0}^N (-1)^j (j+1) \prod_{i=1}^j \left(1 - \frac{i}{N}\right). \quad (\text{D9})$$

We evaluated p numerically for $N = 3 - 1000$. In Fig. 10, we observe that $p = \frac{1}{4} + \mathcal{O}(\frac{1}{N})$. Therefore, our computations suggest that p tends to converge to $\frac{1}{4}$ after initial finite-size effects at $N = 3, 4$.

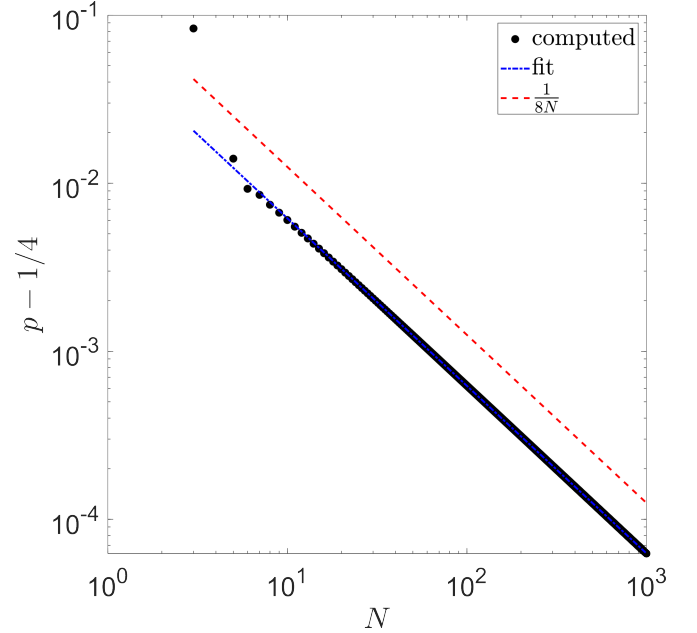


FIG. 10. **Herald probability for N -photon Fourier transform-based distillation schemes.** Excluding $N = 3, 4$, we fit $p - 1/4 = 0.0614 \cdot N^{-0.9973}$.